Multi Objective Design Optimization of Rocket Engine Turbopump Turbine

Naoki Tani , Akira Oyama and Nobuhiro Yamanishi
tani.naoki@jaxa.jp
Japan Aerospace Exploration Agency

JAXA is now planning to develop a next generation booster engine named LE-X, which is a successor of LE-7A. From an engine cycle study, the LE-X requires a high efficiency turbine. To achieve this requirement, a feasibility study of multi-objective design optimization with generic algorithm was applied to the turbine blade shape. The optimized results show strong tradeoff between axial-horsepower and entropy-rise within the stage. By use of Self-Organizing MAP (SOM) and correlation function, it is revealed that this tradeoff is primarily derived from outlet blade design, and inlet blade shape also has an influence to axial-horsepower improvement.

Introduction

In order to achieve high-efficiency and high-robustness, the expander-bleed cycle was chosen as an engine cycle for the next generation booster engine, called LE-X (Fig.1)[1][2]. The LE-X is considered to use the liquid-hydrogen as a fuel, and liquid-oxygen as an oxidizer. The energy source of the turbo-pump driving gas is generated by the heat-exchange around the main combustion chamber in expander-bleed cycle, thus high efficiency pump and turbine are required. According to the engine cycle study, turbine efficiency is more sensitive for the engine total performance compared to pump efficiency [1].

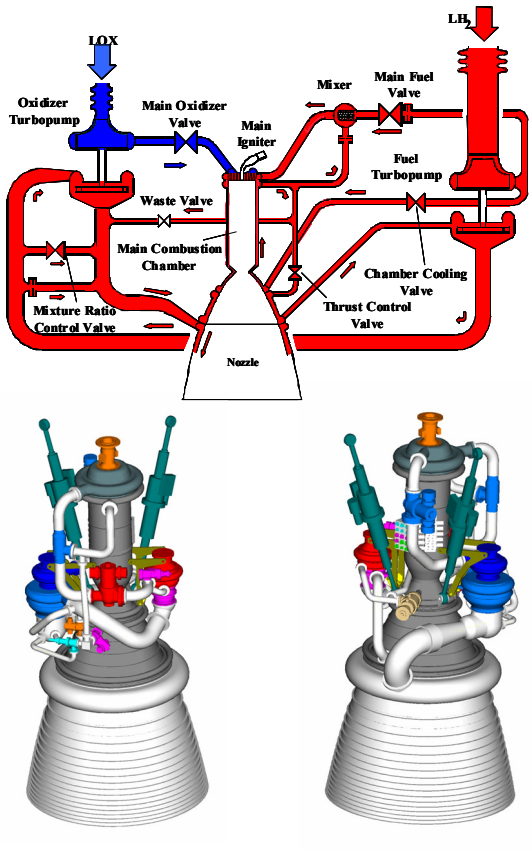

Fig.1 LE-X cycle diagram and 3D model [1]

The shape optimization is considered to be one of the best way to achieve the above objective. Usually, engineering problems are tradeoff problems, such as weight and structural strength. Presently, multi-objective generic algorithm (MOGA) was chosen as an optimization method since MOGA can handle multi objective optimization problem and can search through a large design space. In a gas-turbine, effectiveness of MOGA is widely demonstrated in applications such as a compressor [3], a turbine [4] and a cooling system [5]. However, compared to the gas-turbine, the turbopump turbine is quite highly loaded, therefore, efficiency may not be particularly improved. Therefore, in the present study, to clarify whether the highly-loaded turbine blade can be improved or not, MOGA was applied on a trial base. Usually, it is quite difficult to show trade-off information in MOGA, especially more than three objective functions, so the Self Organizing Map (SOM) was used [6]. SOM can graphically show multi-dimensional trade-off information by projecting to a two-dimensional map.

Table 1 Generic algorithm methods and parameters

Fitness	Pareto Ranking + Shearing
Selection	SUS
Blending	BLX-0.5
Alternation of Generation	Best-N
Mutation Rate	0.1
Generation No.	50
Population No.	16

Computational Method

Multi-Objective Generic Algorithm

The presently used optimization method is a real-coded multi-objective generic algorithm with constraint-handling method by Oyama et al.[7]. One of the features of this

method is more efficient and more robust search of the optimized solution with multiple constraints. The parameters of MOGA are listed in Table 1.

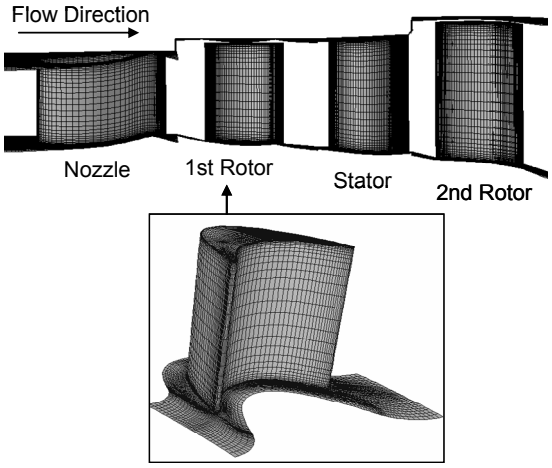

Fig.2 Baseline shape and grid.
The first rotor is selected as an optimization baseline shape

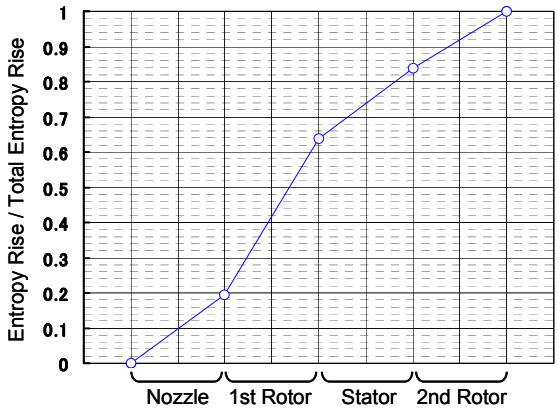

Fig. 3 Entropy rise of each stage
The entropy rise is normalized by total stage entropy rise.

Table 2 Computational conditions

Operating Fluid	Air (Test Rig Condition)
Rotation Speed	14000 rpm
Inlet Boundary Condition	Mass Flow, total Temperature and flow angle are fixed
Outlet Boundary Conditioin	Static pressure is fixed
Space Accuracy	2nd Order Upwind
Pressure-Velocity Coupling	Compressible SIMPLE
Turbulence Model	Realizable k-e

Baseline Shape

The overall and baseline shape of the present optimization is shown in Fig.2, and calculation condition is shown in Table 2. The turbine has two stages, and the first stage rotor is operated in supersonic condition. Figure 3 shows the result of entropy rise of the total stage CFD result. The calculation is at steady condition with a mixing-plane model. The other calculation conditions, such as boundary conditions and turbulence model are the same as the optimization CFD which will be shown later. According to Fig.3, entropy rise of the first stage is the largest, therefore, this stage is selected as an optimization object. The original blade has two-dimensional blade design, however, the blade shape is changed three dimensionally during the optimization process. The turbine performance is expected to be improved by this three dimensionalized blade design.

CFD Setting

As a CFD solver, the commercial code FLUENT 6.3.29 was used. Presently, Mach number in the turbine is considered to be not so high, thus the compressible SIMPLE algorithm was applied with the Pressure-Velocity coupling method. For the advection scheme, second order upwind scheme was applied.

Boundary conditions are important for appropriate optimization, since the operating point may change during the optimization process. Presently, mass flow rate, total temperature and flow angle is set to be constant, and constant static-pressure condition was applied at the outlet boundary condition. For the inlet velocity and temperature and outlet static-pressure distribution, CFD result of total stage calculation was used. The Realizable k-ε model was applied as turbulence model, since the calculated result show the best agreement between experimental results. These conditions are also listed in Table 2.

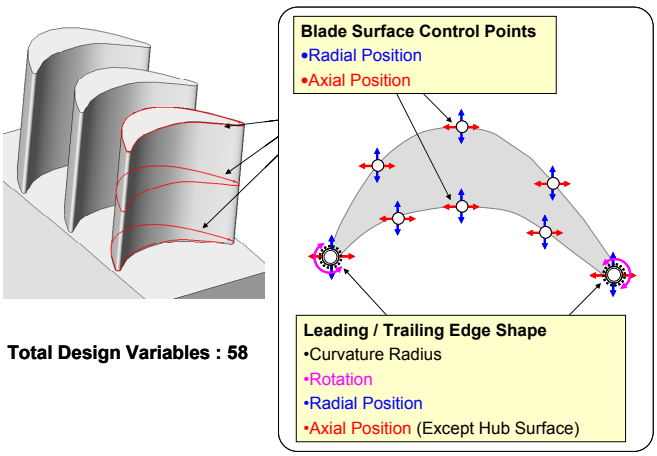

Fig.4 Control points of the design variables

Design Problem

The most important objective of the turbo-pump turbine is to generate torque to drive the pumps with lower fluid loss. In addition, the matching of the following stage is also important from a viewpoint of the total turbine performance. As a result, the following three points are selected as objective functions.

- Axial horsepower **[Axial-Horsepower]: Maximize**
- Entropy rise within the stage
  [Entropy Rise]: Minimize
- Angle of attack(AOA) of the next stage
  [Next Stage AOA]: Minimize

Figure 4 shows control points of the design variables. There are 8 control points in each hub, mean and tip blade section, and each control point moves to the axial and circumferential directions, except the leading and trailing edge control points at the hub. In addition to these two directional movements, scaling and rotating movements were applied to the leading and trailing edge control points. The total design variables are 58. For the shape deformation, grid morphing software SCULPTOR1.8.7 was used. The grid morphing technique has several advantages as follows: one is that complicated grid re-generation method is not necessary, and this method only needs initial grid generation and definition of the control points. The other is a system generality, since shape optimization can be carried out only by defining morphing control points.

Constraint functions are often considered in optimization problem, however, the present optimization is set to be constraint free.

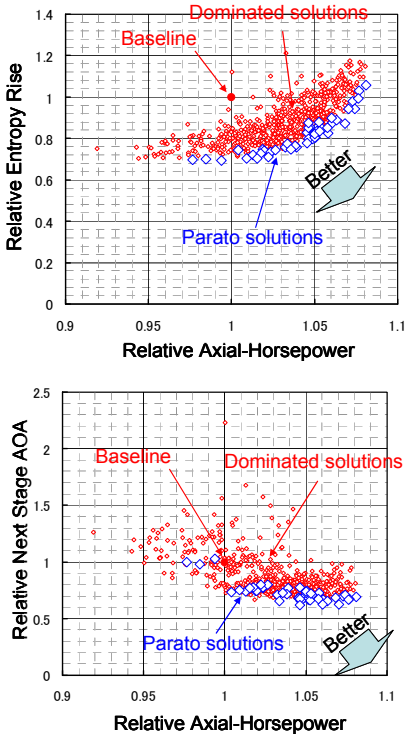

Fig.5 Plots of dominated and parato solutions

Optimized Results

Design Tradeoff

Figure 5 shows the plots of each objective functions of optimization, namely, axial horsepower, entropy rise and next stage AOA. Each value is normalized by the baseline shape result. The maximum improvement of axial-horsepower is about 8% increase, and entropy-rise and next stage AOA are 30% and 40% reduction, respectively. According to Fig.5, it seems that there is a strong correlation between axial horsepower and entropy rise, and a weak correlation between next stage AOA and axial horsepower. However, it is difficult to clarify the relation between design variables and objective functions by these two-dimensional plots. In order to know tradeoff information in multi-objective optimization, Obayashi[6] proposed to use Self-Organizing Map (SOM). The SOM projects multi-dimensional information to two-dimensional surface, and can show tradeoff information more clearly. In addition to SOM visualization, correlation function is used to reveal design tradeoff tendency. The correlation function *Corr* shows the tendency of similarity between two data arrays. If the absolute value of the correlation function is large, correlation between the selected two arrays is strong. And its sign shows tendency.

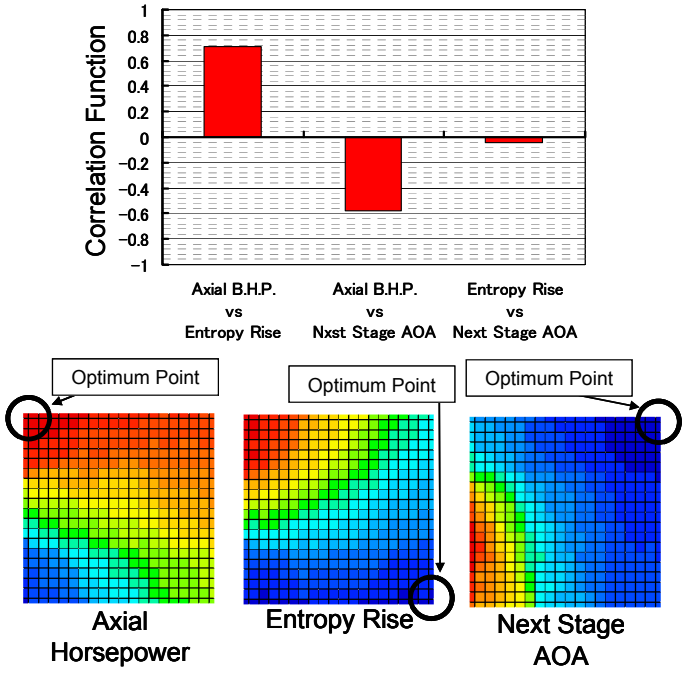

Fig.6 Correlation function (upper) and SOM (lower) of the objective functions

Figure 6 shows SOM and correlation functions of objective functions. According to the Fig. 6, strong tradeoff can be observed between the axial horsepower and the entropy rise,

and the axial horsepower and the next stage AOA. On the contrary, correlation between the entropy rise and the next stage AOA is weak since the correlation function between these two objective functions is small. These results shows that the turbine power output affects internal loss generation (entropy rise) and matching (next stage AOA), but the small internal loss with good matching can be achieved.

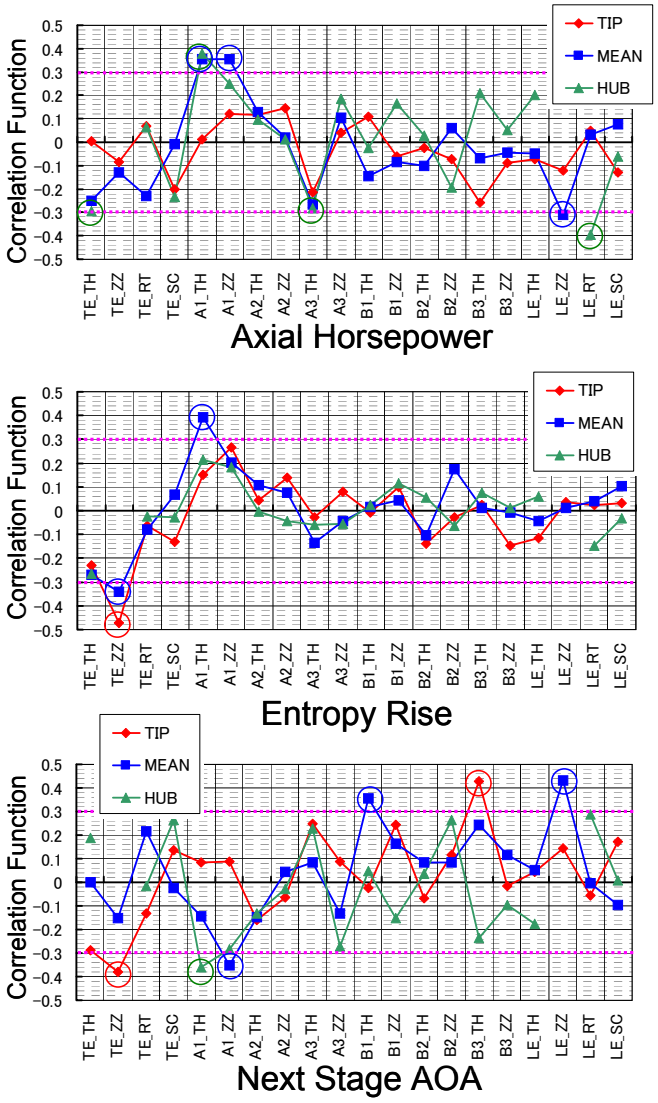

Fig.7 Correlation functions between objective functions and design variables

To clarify the relationship between the objective functions and the design variables, SOM maps and correlation functions survey between objective functions and design variables was also carried out (Fig.7). In Table3, the design variables which have strong correlation to each objective functions are shown. The positions of each design variables and SOM are shown in Figure 8. According to Fig.7 and 8, trailing edge design variables take an important role to the entropy rise, and the axial horsepower and the AOA of the next stage is strongly affected by both the leading and the trailing edge design variables. Also, pressure surface design has little influence to each objective function

Table3 Design variables which have large correlation functions. The present threshold is $|Corr| \geq 0.3$

Objective Function	Cross Section	Design Variable
Axial Horsepower	MEAN	A1_TH A1_ZZ LE_ZZ
	HUB	TE_TH A1_TH LE_RT
Entropy Rise	TIP	TE_ZZ
	MEAN	TE_ZZ A1_TH
Next Stage AOA	TIP	TE_ZZ B3_TH
	MEAN	A1_ZZ B1_TH LE_ZZ
	HUB	A1_TH

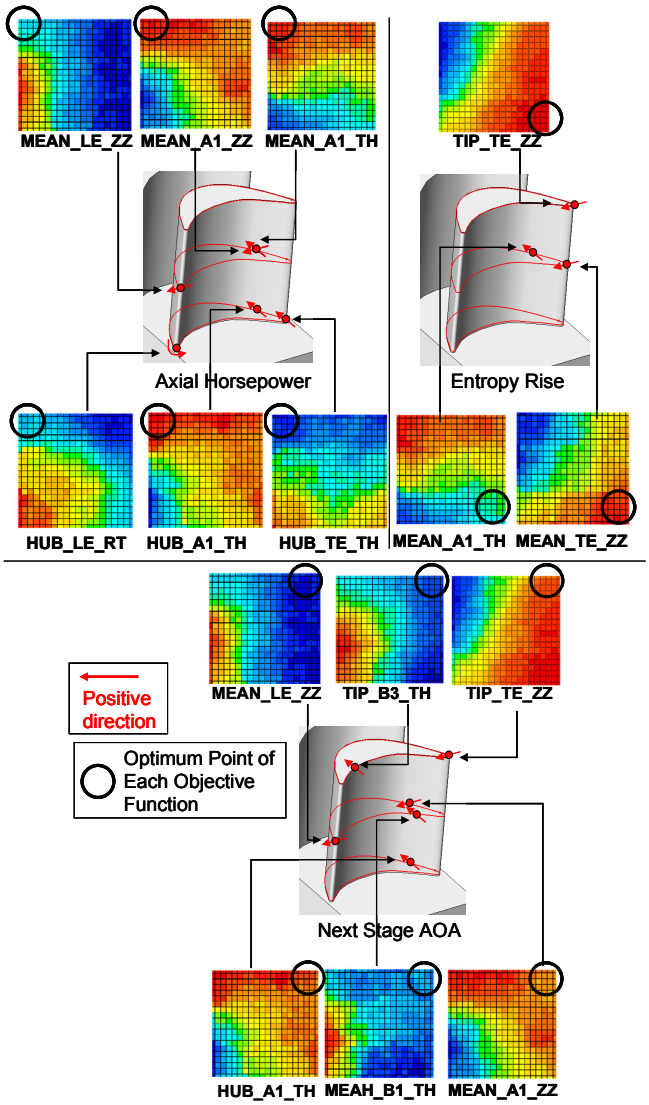

Fig.8 Design variables and SOM which have strong correlation to each objective function

Internal Flow

In this section, the relation between internal flow and design tradeoff is considered. According to Fig. 5, the next stage AOA does not greatly change compared to the other two objective functions. Therefore, consideration of tradeoff between axial horsepower and entropy rise is mainly mentioned.

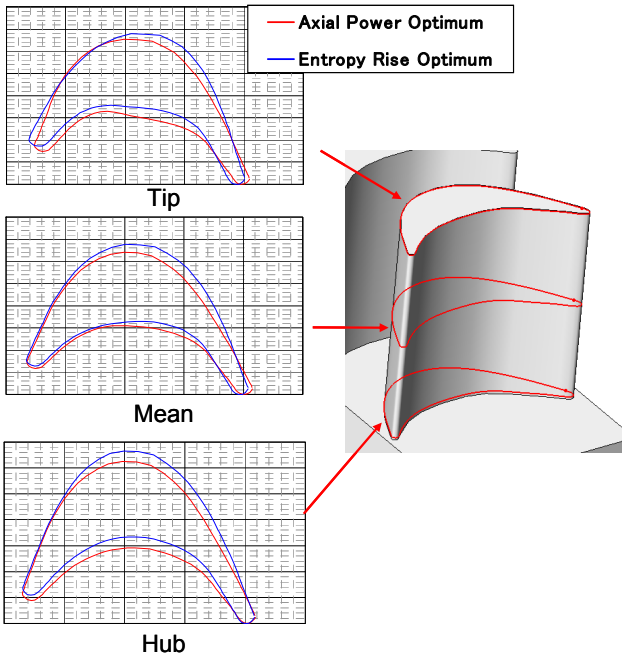

Fig.9 Blade shape of each cross section

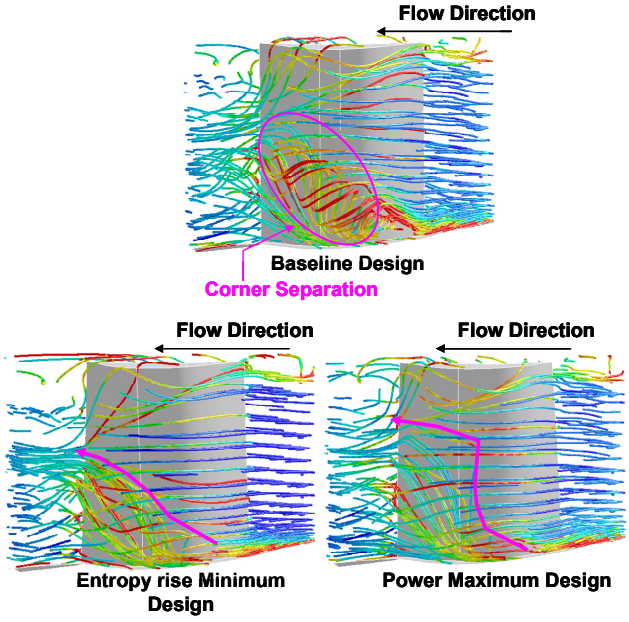

Fig.10 Pathlines colored by vorticity magnitude

Figure 9 and 10 respectively show blade shape and the pathlines of the each optimum result. It can be observed that corner separation at the blade suction side is reduced in both of the optimized results. And corner separation of the entropy-rise optimum solution becomes even smaller than that of the other two results. According to these results, the corner separation takes an important role to reduce entropy rise within the stage.

The corner separation occurs at the hub and tip around the mid-chord position. To reduce the entropy-rise, the separation region must be discharged before its development. One of the best ways for accelerate discharge is to increase the flow velocity. According to the correlation study and blade shape comparison, which are shown in Fig.8 and 10, respectively, increase of velocity is achieved by increasing the outlet blade angle. This is consistent to Table 3 that the trailing edge control points have strong influence to the entropy-rise.

From here, consideration of axial-horsepower optimum result will be carried out. According to the ideal velocity triangle study, turbine output horsepower can be estimated as following.

$$Power = U \cdot \Delta U \cdot m \qquad (1)$$

Where, Power, U, ΔU and *m* are axial-horsepower, rotation speed, tangential velocity difference in the stage and mass flow rate, respectively. In the present calculation, inlet mass flow, flow angle and rotation speed is set to be constant, therefore, tangential velocity difference is the major cause of output horsepower difference. Figure 11 shows pressure, temperature, velocity and other physical values comparison between entropy-rise optimum and axial-horsepower optimum results. According to Fig.11, the inlet tangential velocity magnitude of axial-horsepower optimum result becomes larger than that of entropy-rise optimum result. On the contrary, at the outlet, the tendency of the tangential velocity magnitude becomes reverse, however, the difference at the inlet is larger than that of the outlet. Therefore, it can be said that inlet velocity increase takes an important role for axial-horsepower improvement. In order to increase the inlet velocity, the density should become lower, and Fig.11 shows that this density reduction is mainly derived from the inlet pressure reduction. One of the answers to reduce the inlet pressure is to minimize the inlet flow incidence. Therefore, it seems that the following two design variables affect the above consideration.

- MEAN_LE_ZZ, HUB_LE_RT

From a viewpoint of the improvement of the axial-horsepower, the outlet tangential velocity is also important to achieve large ΔU. The trailing edge design variables, which are described below, have also influence to the axial-horsepower.

- MEAN_A1_TH, MEAN_A1_ZZ, MEAN_LE_ZZ, HUB_TE_TH, HUB_A1_TH

Some of these variables have correlation to entropy-rise

according to the above discussion and Table 3.

In summary, the inlet blade angle affects axial-horsepower improvement by increasing inlet velocity. And the outlet blade design influences both axial-horsepower and entropy-rise by controlling corner separation.

Summary

In the present study, multi-objective shape optimization of turbine blade was carried out. The objective functions are axial-horsepower, entropy-rise, and outlet flow angle. The conclusions of the study are followings.

- The MOGA is effective in the optimization of highly-loaded rocket turbine blades.
- Both entropy-rise and outlet flow angle have strong correlation to axial-horsepower, but correlation between entropy-rise and outlet flow angle is weak.
- The inlet blade design primarily influences to axial-horsepower improvement.
- The outlet blade design influences all objective functions by controlling the corner separation.

In the present study, confirmation of the total stage performance improvement was not carried out, and this work remains as one of the future studies.

Acknowledgement

The present work is carried out in the LE-X research program. The authors greatly acknowledge to IHI co. ltd., which manufactures the turbo-pump, Dr. K. Chiba, who is a specialist of optimization, and JAXA Space Transportation Mission Directorate.

References

[1] Kurosu, A., et al., “Study of Next Booster Engine LEX in Japan,” AIAA2006-4700, 2006

[2] Negoro, N., et al., “Next Booster Engine LE-X in Japan”, AIAA2007-5490, 2007

[3] Oyama, A., et al., "Transonic Axial-Flow Blade Optimization Using Evolutionary Algorithms and a Three-Dimensional Navier-Stokes Solver," AIAA Journal of Propulsion and Power, Vol. 20, No. 4, pp. 612-619, 2004

[4] Griffin, L.W., et al., “Design and Analysis of Turbines for Space Applications,” AIAA2003-3993, 2003

[5] Schumacher, T., Weston, T. and Campos, F., “Automatic Optimisation of Aircraft Ventilation System Components with CFD,” IACC2007, 2007

[6] Obayashi, S., Jeong, S. and Chiba, K., “Multi-Objective Design Exploration for Aerodynamic Configurations,” AIAA2005-4666, 2005

[7] Oyama, A, Shimoyama, K. and Fujii, K., “New Constraint-Handling Method for Multi-Objective and Multi-Constraint Evolutionary Optimization,” Transactions of the Japan Society for Aeronautical and Space Sciences, Vol.50, Vol.157, pp.56-62, 2007

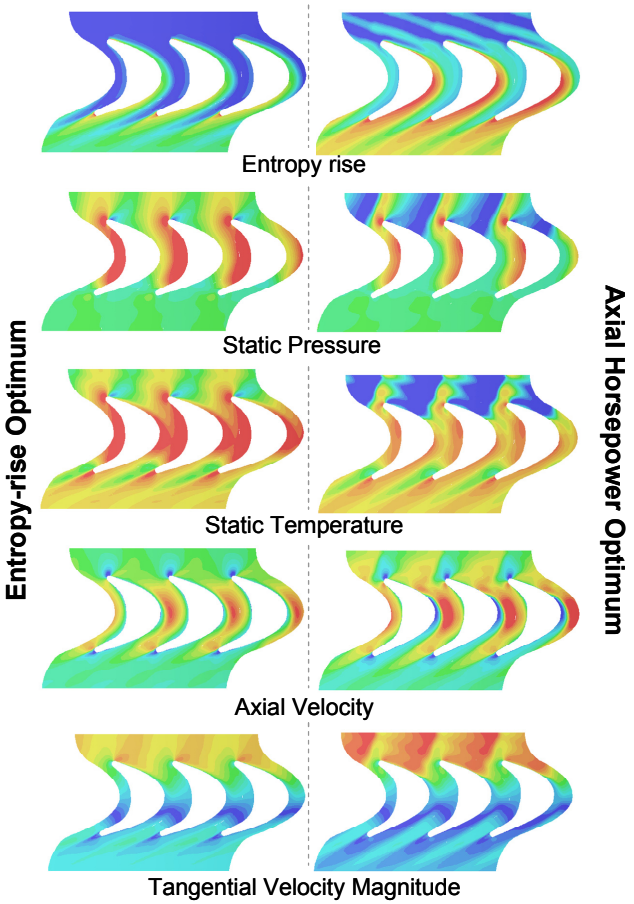

Fig.11 Physical value distribution at mean section